International Journal of Mass Spectrometry 197 (2000) 123–130

Comparison of high-field ion mobility obtained from drift tubes and a FAIMS apparatus

Larry A. Viehland[a,1], Roger Guevremont[b,*], Randy W. Purves[c], David A. Barnett[b]

[a]Department of Chemistry, Saint Louis University, St. Louis, MO 63103, USA
[b]Institute for National Measurement Standards, National Research Council of Canada, Ottawa, ON K1A 0R6, Canada
[c]PE Sciex, 71 Four Valley Drive, Concord, ON L4K 4V8, Canada

Received 6 August 1999; accepted 27 September 1999

Abstract

High-field asymmetric waveform ion mobility spectrometry (FAIMS) separates ions by application of a high-voltage asymmetric waveform to closely spaced electrodes such that ions experience (transient) electric fields that are sufficiently high that the mobility deviates from its low field limit. We describe the use of FAIMS to determine the mobility of the chloride ion, *m/z* −35, at ~760 Torr and ~300 K in fields up to ~65 Td. The high-field mobility of chloride was determined from FAIMS data using linear and nonlinear least squares techniques, and was found to agree well with published values of mobility determined by drift tube systems up to 50 Td. (Int J Mass Spectrom 197 (2000) 123–130) © 2000 Elsevier Science B.V.

Keywords: Ion mobility; FAIMS

1. Introduction

Ion mobility spectrometry (IMS) has become an important technique for the analysis of many compounds, due to high sensitivity, amenability to miniaturization, and ruggedness in operation. A conventional IMS provides ion mobility values in the limit of low *E/N*, the ratio of the electric field strength (E) to the gas number density (N). Most commercial IMS systems are not designed to operate at higher *E/N* values in which the ion mobility deviates measurably from the low-field limit.

The dependence of ion mobility on *E/N* provides important information about the ion-neutral interaction potential. To obtain such information, IMS techniques have recently been extended [1–4] to incorporate a pair of cylindrical plates creating a nonuniform electric field that can operate at high *E/N*, and a transverse, variable electric field to achieve separation of the ions. This technique is referred to as high-field asymmetric waveform ion mobility spectrometry or FAIMS. Recently, a FAIMS device was characterized using mass spectrometric detection (FAIMS-MS) [2].

2. Instrumentation

Electrospray ionization-FAIMS-mass spectrometry (ESI-FAIMS-MS) experiments were performed using a PE Sciex API 300 triple quadrupole mass

---

* Corresponding author.

[1] Present address: Division of Science, Chatham College, Pittsburgh, PA 15232.

1387-3806/00/$20.00 © 2000 Elsevier Science B.V. All rights reserved
PII S1387-3806(99)00224-9

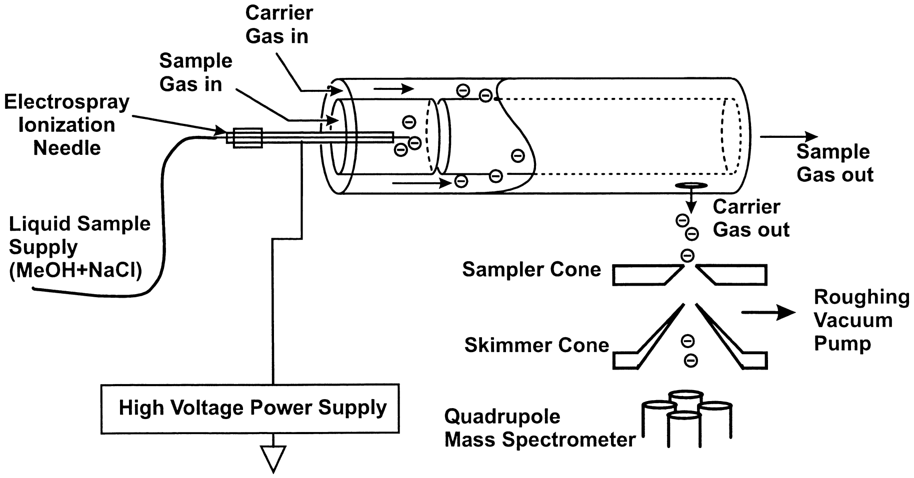

Fig. 1. Three-dimensional schematic of the ESI-FAIMS-MS system. Gaseous chloride ions are generated in the short inner cylinder via electrospray ionization of a dilute methanolic solution of NaCl.

spectrometer (PE Sciex, Concord, ON). A three-dimensional view of the ESI-FAIMS-MS instrument used in this study is shown in Fig. 1 and in cross section in Fig. 2. Ions were transferred to the vacuum chamber of the mass spectrometer through a "sampler cone" placed at the end of the FAIMS analyzer at a 45 ° angle relative to the axis of the FAIMS cylinders. (For clarity, the ESI-FAIMS-MS shown schematically in Fig. 1 shows the ions exiting the FAIMS at a 90° angle.) The diameter of the orifice in the sampler cone was ~260 μm.

The FAIMS ion filter shown in Fig. 1 was composed of two inner cylinders, which were axially aligned and positioned ~5 mm apart, and an outer cylinder that surrounded the two inner cylinders [2]. The outer cylinder and the short inner cylinder of the

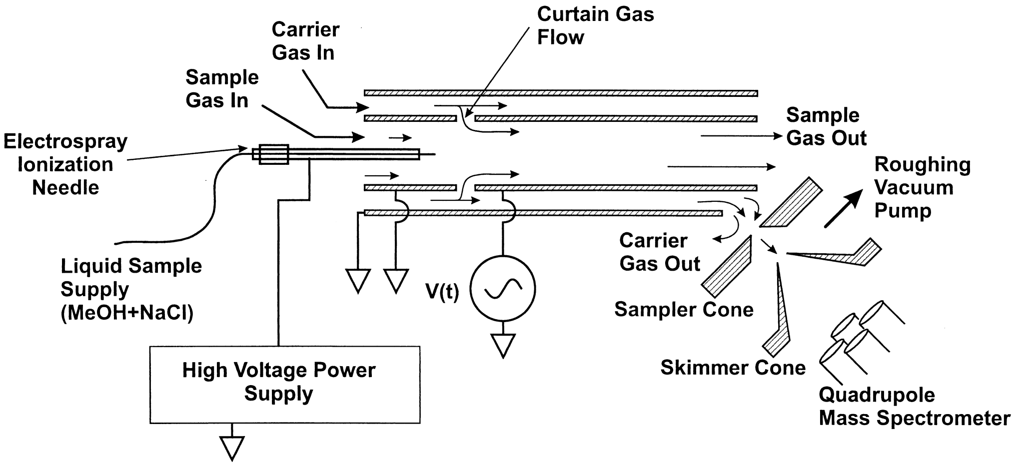

Fig. 2. Cross section of the ESI-FAIMS-MS system. The gas flows are adjusted such that a portion of the "Carrier In" flow acts as a "curtain" gas to assist in ion desolvation and to prevent contamination of the analyzer region.

FAIMS instrument were held at the same electrical potential. The long inner cylinder had a high frequency (210 kHz), high voltage (up to 4950 V *p-p*), asymmetric waveform applied to it, thereby establishing the electric field between the inner and outer tubes. The peak voltage during this waveform is called the "dispersion voltage" (D). In addition to this high frequency waveform, a low dc voltage, called the "compensation voltage" (C) was also applied to the long inner cylinder.

The electrospray needle was placed on the center axis of the short inner cylinder, terminating ~5 mm short of the gap between the two inner cylinders. ESI generated ions were driven radially outward by the electric field to the analyzer region through the 5 mm gap between the two inner cylinders. For the generation of chloride ions, the electrospray needle was held at ~ −1950 V, giving an electrospray current of ~ −45 nA.

Gas connections to the FAIMS system are also shown in Figs. 1 and 2. Compressed air was passed through a gas purification cylinder (charcoal/molecular sieve) and introduced into the FAIMS device. Gas entered through the Carrier In (C_{in}) port, and exited via the Carrier Out (C_{out}) and Sample Out (S_{out}) ports. All three flows could be adjusted independently. In this study, the gas was introduced through C_{in} at a flow rate of 5 L/min. The gas exited through S_{out} at 1 L/min and through C_{out} at 4 L/min. A fraction of the input flow, directed radially inward through the 5 mm gap between the inner cylinders, shown in Fig. 2, acted as a curtain gas. While the ions formed by ESI were driven radially outward through the gap by the electric field, the curtain gas prevented neutrals from entering the annular analyzer region. The curtain gas is particularly important for FAIMS separation of low mass ions (whose mobilities increase at high field) because the separation of these ions is very susceptible to the effects of carrier gas contamination [2,4]. The curtain gas portion of the input flow, along with the neutrals, exited the FAIMS device via S_{out}. The remainder of the gas flow carried the electrospray ions along the length of the annular space between the outer cylinder and the long inner cylinder.

The mass spectrometer orifice was electrically insulated from the FAIMS device and a separate voltage of −24 V was applied to it. An offset voltage of −49 V was applied to the entire FAIMS unit to enhance the sensitivity of the FAIMS-MS.

The pressure in the FAIMS system was measured using a MKS Baratron Model 170M-6B and pressure sensing head type 3TOBJ-1000 connected to the Sample In (S_{in}) port (MKS Instruments, Boulder, CO). There was no gas flow through the S_{in} port in this study. The reference inlet to the differential pressure sensing head was at atmospheric pressure. Atmospheric pressure was measured with a mercury barometer.

3. Results and discussion

3.1. The ideal square wave asymmetric waveform

The principles of operation of FAIMS have been described by Buryakov et al. [5] for a device consisting of two parallel plates, with one kept at ground potential while an asymmetric waveform was applied to the other. The waveform $V(t)$ was composed of a brief high voltage component lasting for time t_{high}, and a low voltage component of opposite polarity lasting for a longer period of time t_{low}. The integrated voltage-time product of one complete cycle of the waveform was equal to zero.

An anion (e.g., chloride ion) that is transported by a gas stream between the two parallel plates will oscillate between the plates as illustrated in Fig. 3. During the high-field portion of the waveform $V(t)$ the field will cause the ion to move with velocity

$$v_{high} = K_0 E_{high} \tag{1}$$

where E_{high} is the applied field and K_0 is the high-field ion mobility. The distance traveled by the ion during application of the field is

$$d_{high} = v_{high} t_{high} = K_0 E_{high} t_{high} \tag{2}$$

Similarly the ion travels a distance of

$$d_{low} = v_{low} t_{low} = K_0^{(low)} E_{low} t_{low} \tag{3}$$

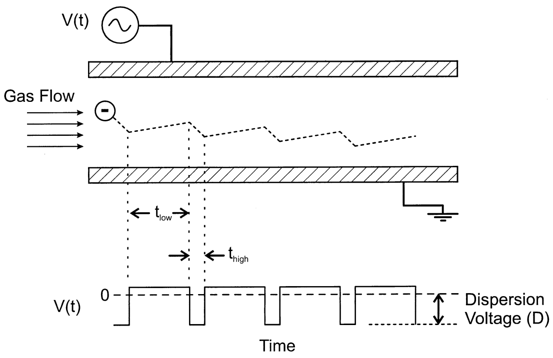

Fig. 3. Motion of a negatively charged ion in a flat-plate FAIMS during application of a hypothetical asymmetric square wave having low and high voltage time periods t_{low} and t_{high}, with a ratio $t_{\text{low}}/t_{\text{high}}$ of ~4. The peak voltage D is approximately -3000 V, with plate spacing ~2 mm. The motion of a negative ion whose mobility increases at high electric field is illustrated by the dashed line.

during the longer portion of the waveform at which time the opposite polarity electric field is weak enough that the ion mobility $K_0^{(\text{low})}$ is closer to its zero-field limiting value $K_0^{(0)}$. If E_{high} is sufficiently strong such that K_0 is appreciably higher than $K_0^{(\text{low})}$, the distance traveled by the ion during t_{high} is then greater than the distance traveled during t_{low}. The ion, therefore, experiences a net displacement toward the lower plate as illustrated by the dashed line in Fig. 3.

If a negative ion such as chloride experiences a net migration way from the upper plate, a constant positive dc voltage may be applied to this plate to reverse or "compensate" for the drift so that the ion has no net motion toward either plate. This dc voltage is referred to as the compensation voltage (C). If two ionic species respond differently to the applied electric field (i.e., their K_0 to $K_0^{(\text{low})}$ ratios are not identical) the C required to prevent their drift toward either plate will also differ, thereby allowing selective transport of one ion over the other.

At the C and D of optimum transmission of an ion, the magnitude of the distances d_{high} and d_{low} described by Eqs. (2) and (3) will be equal. The ratio of K_0 to $K_0^{(\text{low})}$ can therefore be determined from the electric fields and the time periods of the asymmetric waveform. If during the high and low voltage portion of $V(t)$, the mobility is K_0 and $K_0^{(\text{low})}$, respectively, then:

$$\frac{K_0}{K_0^{(\text{low})}} = \frac{D - C(t_{\text{low}}/t_{\text{high}})}{D + C} \tag{4}$$

where C and D correspond to conditions of maximum ion transmission. For chloride ions, D is negative and C is positive, and the ratio described by Eq. (4) is >1.

Some analysis of Eq. (4) is necessary to evaluate the possible use of a square wave asymmetric waveform in the FAIMS apparatus for determination of the ratio of high- to low-field mobility of an ion. The conditions of large and small ratios of t_{low} to t_{high} are quite distinct.

A large ratio of t_{low} to t_{high} would seem, intuitively, to maximize the difference in electric field conditions during the high- and low-field portions of the square-wave asymmetric waveform, making $K_0^{(\text{low})}$ equal to $K_0^{(0)}$ and maximizing the difference between K_0 and $K_0^{(0)}$. Unfortunately, Eq. (4) also suggests that increasing the ratio of t_{low} to t_{high} has the undesirable side effect of decreasing the experimentally observed compensation voltage C.

A small ratio of t_{low} to t_{high} (i.e., ratio of t_{low} to t_{high} approaches 1:1) means that the high and low voltage periods of the waveform converge to equal voltage, and therefore the value of $K_0^{(\text{low})}$ approaches K_0 rather than $K_0^{(0)}$. Since the difference in mobility between the high- and low-voltage periods of the waveform disappears, the experimentally measured C approaches zero. The highest C that is experimentally observed falls between these extremes of large and small ratio of t_{low} to t_{high}. Numerical modeling of the ion trajectory indicates the maximum measured compensation voltage occurs when the t_{low} to t_{high} ratio is ~2:1.

3.2. Transient effects

The previous section ignored the effects that will occur during the time it takes for the ion to respond to the idealized square-wave asymmetric waveform. The equations assumed that the ion has reached "steady state" drift velocity immediately after the abrupt change in the applied electric field. Fortunately, velocity and energy relaxation of ions in drift tubes has been studied by Lin et al. [6] in the context of "ping-pong" experiments [7,8]. This theory showed that, to first order, the time for reaching terminal velocity could be neglected if τ is small relative to the total drift time t. This ratio of τ/t can be estimated using:

$$\frac{2mv_d}{qEt} = \frac{2mK}{qt} \equiv \frac{\tau}{t} \tag{5}$$

where m and q are the ion mass and charge. Long after the transients have died out and the electric field intensity has stabilized at E, the ion drift velocity, v_d, is related to the ion mobility K by

$$v_d = KE = N_0 K_0(E/N) \tag{6}$$

where N_0 is Loschmidt's constant, the number density of a gas at STP. A worst case estimate of the relaxation time may be calculated by choosing $q = 1.602 \times 10^{-19}$ C, $m = 1 \times 10^{-26}$ kg, $K = 3$ cm^2/V s, which gives

$$\tau \approx 4 \times 10^{-11} \text{ s} \tag{7}$$

Since the field reversals in a FAIMS experiment occur within a time frame of 1–20 μs, the relaxation time is sufficiently short that the fractional error due to the neglect of transients can be ignored.

3.3. The actual asymmetric waveform

The constraints placed on power consumption of the electronic circuitry force existing FAIMS instruments to operate using waveforms synthesized by summation of a sine (or cosine) wave and a harmonic, rather than the ideal square-wave asymmetric waveform described above. The total electric field as a function of time at a location equidistant between the plates is approximated by:

$$E(t) = \frac{3C + 2D\sin(\omega t) + D\sin(2\omega t - \pi/2)}{3d} \tag{8}$$

where d is the distance between the cylindrical plates, C is the compensation voltage, D is the dispersion high voltage, and ω is the angular frequency.

During application of the waveform the mobility of the ion responds to the changing electric fields, when E/N is not too large and N is constant, as:

$$K_0(t) = K_0^{(0)} \sum_{k=0}^{\infty} c_k E^{2k}(t) \tag{9}$$

where $c_0 = 1$. We let $\theta = \omega t$ and note that the drift velocity is the product of the ion mobility and the electric field. Therefore the criterion that the ions experience no net motion during one full cycle of the waveform reduces to the requirement that

$$\sum_{k=0}^{\infty} c_k \int_0^{2\pi} E^{2k+1}(\theta)\, d\theta = 0 \tag{10}$$

Note that it is this criterion of no net ionic motion that justifies, to first order, the neglect in Eq. (8) of a possible dependence of the electric field on radial location.

It can be shown from Eq. (8) that Eq. (10) is equivalent to the requirement that

$$\sum_{k=0}^{\infty} \frac{c_k}{d^{2k}} \sum_{l=0}^{2k+1} G_l \binom{2k+1}{l} C^{2k+1-l} D^l = 0 \tag{11}$$

where the parentheses represent a binomial coefficient and where

$$G_l = \frac{1}{3^l} \sum_{m=0}^{l} (-1)^{l-m} 2^m \binom{l}{m} \sum_{n=0}^{m}{}' \frac{1}{2^{m+n}} \binom{m}{n} \cdot \binom{m+n}{(m+n)/2} \tag{12}$$

The prime in this equation indicates that the only terms retained in the sum have $m + n$ even.

3.4. Power series for the mobility

Use of Eq. (11) involves the least-squares determination of the coefficients c_k for systematically

Table 1
ESI-FAIMS-MS data for $^{35}Cl^-$ ions in air

D (V)	C (V)	Maximum E/N (Td)	D (V)	C (V)	Maximum E/N (Td)
0	−0.03	0.00	−1700	5.80	34.60
−500	0.04	10.21	−1800	7.20	36.62
−600	0.11	12.25	−1900	8.80	38.63
−700	0.25	14.29	−2000	10.60	40.63
−800	0.50	16.33	−2100	13.00	42.63
−900	0.67	18.37	−2200	15.60	44.62
−1000	1.00	20.40	−2300	18.70	46.60
−1100	1.36	22.44	−2500	25.20	50.55
−1200	1.78	24.47	−2700	34.00	54.45
−1300	2.33	26.50	−2900	42.50	58.36
−1400	3.00	28.53	−3100	52.40	62.25
−1500	3.75	30.56	−3300	61.20	66.15
−1600	4.70	32.58			

larger values of k. It is analogous therefore, to using equation-of-state data to determine successively higher virial coefficients. To illustrate this method, we will consider experimental results for $^{35}Cl^-$ ions in air (pressure of 760 Torr, temperature of 300 K, and number density of 2.45×10^{19} cm^{-3}) obtained with an annular space of $d = 2.0$ mm in the FAIMS apparatus. The value C of the compensation voltage needed to prevent ion motion at each value D of the high-voltage portion of the asymmetric waveform is given in Table 1, along with the maximum value of the reduced field strength E/N obtained from Eq. (8) and the known number density of the gas.

If we keep only the $k \leq 2$ terms in Eq. (11), we can rearrange the resulting equation as

$$y = c_1 + mc_2 \tag{13}$$

with

$$y = \frac{-Cd^2}{C^3 + \frac{5}{6}CD^2 + \frac{1}{9}D^3} \tag{14}$$

and

$$m = \frac{C^5 + (25/9)C^3D^2 + (10/9)C^2D^3 + (55/72)CD^4 + (55/486)D^5}{d^2(C^3 + (5/6)CD^2 + (1/9)D^3)} \tag{15}$$

A linear least-squares fit can be used to estimate c_1 and c_2. In practice, however, the results depend sensitively upon whether all or only a subset of the data in Table 1 is analyzed. This is because of the limited number of significant figures available for C at low D and because of the influence of terms with $k > 2$ in Eq. (11) at high D. Consequently, low and high D values are systematically removed until a situation is reached where the least-squares fit gives a minimum 95% confidence interval for the intercept. In this case data from $D = -900$ to -3100 V gave $c_1 = (1.87 \pm 0.09) \times 10^{-5}$ (cm/V)^2.

To obtain c_2, the terms with $k \leq 3$ are retained in Eq. (11), and it is assumed that c_1 has the value just determined. The equation is rearranged such that c_2 is the intercept of a linear least-squares plot while low D and high D values are again systematically removed to minimize the 95% confidence interval for the intercept. This approach gave $c_2 = (6.44 \pm 0.46) \times 10^{-9}$ (cm/V)^4. Repeating this process a third time gave $c_3 = (-3.80 \pm 4.45) \times 10^{-13}$ (cm/V)^6. The high uncertainty associated with this value indicates that it would be pointless to proceed to higher k values in Eq. (11).

Fig. 4 shows a comparison between the ESI-FAIMS-MS values (dashed curves) obtained in the

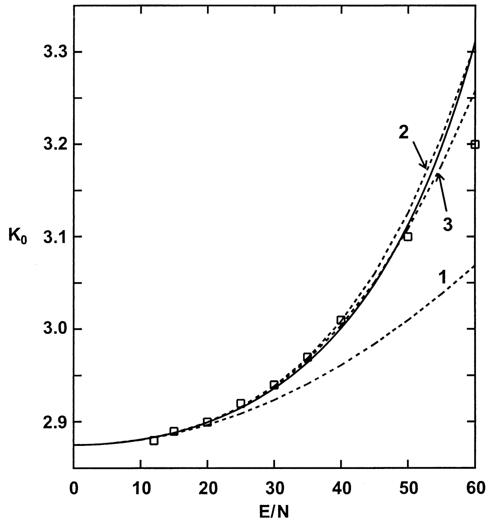

Fig. 4. Mobilities, K_0 in cm^2/V s as a function of the reduced electric field strength, *E/N* in Td, for $^{35}\mathrm{Cl}^-$ in air at 300 K and 760 Torr. The solid curve is obtained using a nonlinear function for K_0 (*E/N*) and adjusting the parameters to match the FAIMS data. The dashed curves were obtained from the FAIMS data using an expansion of K_0 in powers of $(E/N)^2$, truncated to the number of coefficients c_k indicated by the label on the curve. The points are values from Ref. 9 that were obtained by conventional drift-tube techniques.

manner just described, with successively higher k terms retained in Eq. (11), and the values (squares) of the mobility of chloride ions in air at 295.5 K obtained by conventional drift-tube methods [9]. The agreement with $k = 3$ is excellent up to 50 Td, i.e., approximately the highest *E/N* value probed by the FAIMS experiments. However, it must be noted that when using the coefficients c_k in Eq. (9) to obtain K_0, it was necessary to assume that the zero-field mobility had the value 2.875 cm^2/V s. Although it is possible in principle to obtain $K_0^{(0)}$ from an ESI-FAIMS-MS experiment with a real asymmetric waveform (but not an ideal one! [10]), accurate values are unlikely to be realized unless more data is taken at low D values and unless the corresponding C values can be determined with higher precision.

3.5. Nonlinear functional form for the mobility

An alternative way to analyze the FAIMS data is to match it to a nonlinear functional form for the mobility, one that applies to higher *E/N* than the power series expansion presented above, even if it is not as theoretically well-founded. Although it has not been used much in recent years, such a functional form does exist [11,12]. It is

$$K_0\left(\frac{E}{N}\right) = K_0^{(0)}\left[1 + b_1\left(\frac{E}{N}\right)^2\right]^{1/4} \times \left[1 + b_2\left(\frac{E}{N}\right)^2 + b_3\left(\frac{E}{N}\right)^4\right]^{-1/4} \times \left[1 + a_1\left(\frac{E}{N}\right)^2 + a_2\left(\frac{E}{N}\right)^4\right]^{-1/8} \quad (16)$$

The criterion that the ions will experience no net motion during one full cycle of the FAIMS waveform is that

$$\int_0^{2\pi} K_0[E(\theta)]E(\theta)\, d\theta = 0 \quad (17)$$

where the electric field is given by Eq. (8) and where $E(\theta)$ is used as the argument in Eq. (16) rather than *E/N*. The nonlinear least-squares problem is to choose the five parameters in Eq. (16) so that

$$S_0 \equiv \sum_i \int_0^{2\pi} K_0[E_i(\theta)]E_i(\theta)\, d\theta \quad (18)$$

has a minimum value; the subscript i on the electric field indicates that a particular pair of experimental values are used for C and D in Eq. (8). The necessary five nonlinear equations are obtained by differentiating Eq. (18) with respect to each of the five unknowns successively, and setting the partial derivatives equal to zero. A computer program (Fortran-90, Visual Basic) has been written to implement this nonlinear, least-squares procedure and was used to analyze the data in Table 1. To six significant figures, the parameters of Eq. (16) obtained in this way are given in Table 2. The mobilities obtained by using these parameters in Eq. (16) are shown in Fig. 4 (solid line) to be in excellent agreement with both the values from Ref. 9 and with the values obtained by assuming a power series expansion for K_0.

Table 2
The parameters of Eq. (16) for $^{35}Cl^-$ ions in air

a_1	-4.83016×10^{-5}	Td^{-2}
a_2	-1.62365×10^{-8}	Td^{-4}
b_1	2.75541×10^{-5}	Td^{-2}
b_2	-2.55173×10^{-5}	Td^{-2}
b_3	-8.61896×10^{-9}	Td^{-4}

4. Summary

The ESI-FAIMS-MS apparatus has been demonstrated to be an accurate way of determining the high-field mobility of ions in gases. Although it uses atmospheric pressure gases rather than the low pressures used in conventional drift tubes, the *E/N* range covered by this apparatus reaches to at least 50 Td. Moreover, mobility data can be obtained quickly for a wide array of ions because the apparatus is easily coupled to a corona discharge or electrospray ion source and because a mass spectrometer can be used as the ion detector.

References

[1] B.L. Carnahan, A.S. Tarassov, U.S. Patent No. 5420424 (1995).
[2] R.W. Purves, R. Guevremont, S. Day, C.W. Pipich, M.S. Matyjaszczyk, Rev. Sci. Instrum. 69 (1998) 4094.
[3] E.V. Krylov, Tech. Phys. 44 (1999) 113.
[4] R. Guevremont, R.W. Purves, Rev. Sci. Instrum. 70 (1999) 1370.
[5] I.A. Buryakov, E.V. Krylov, E.G. Nazarov, U.Kh. Rasulev, Int. J. Mass Spectrom. Ion Processes 128 (1993) 143.
[6] S.L. Lin, L.A. Viehland, E.A. Mason, J.H. Whealton, J.N. Bardsley, J. Phys. B 17 (1977) 3567.
[7] J. Heimerl, R. Johnsen, M.A. Biondi, J. Chem. Phys. 51 (1969) 5041.
[8] R. Johnsen, M.A. Biondi, J. Chem. Phys. 57 (1972) 1975.
[9] H. Bohringer, D.W. Fahey, W. Lindinger, F. Howorka, F.C. Fehsenfeld, D.L. Albritton, Int. J. Mass Spectrom. Ion Processes 81 (1987) 45.
[10] L. Viehland, unpublished results.
[11] M. Saporoschenko, Phys. Rev. A 8 (1973) 1044.
[12] F. Li-Aravena, M. Saporoschenko, J. Chem. Phys. 98 (1993) 8888.